Mapping the network architecture of gap junctional coupling among parallel processing channels in the mammalian retina

Crystal L. Sigulinsky[1], James R. Anderson[1], Ethan Kerzner[2], Christopher N. Rapp[1], Rebecca L. Pfeiffer[1], Daniel P. Emrich[1], Kevin D. Rapp[1], Noah T. Nelson[1], J. Scott Lauritzen[1], Miriah Meyer[2], Robert E. Marc[1], Bryan W. Jones[1]

[1]Department of Ophthalmology, John A. Moran Vision Institute, University of Utah School of Medicine, Salt Lake City, Utah, USA.
[2]Scientific Computing and Imaging Institute, University of Utah School of Computing, Salt Lake City, Utah, USA.

1. Introduction.

Electrical synapses are fundamental components of neural networks. Gap junctions provide the anatomical basis for electrical synapses and are prevalent throughout the neural retina with essential roles in signal transmission. Gap junctions within and between the parallel processing channels afforded by retinal bipolar cells have been reported or predicted, but their roles, partners, and patterns remain largely unknown. Here, we took advantage of the high resolution of Retinal Connectome 1 (RC1) to reconstruct ON cone bipolar cells (CBCs) and map their coupling topologies.

2. Reconstructing morphology and synaptology in RC1.

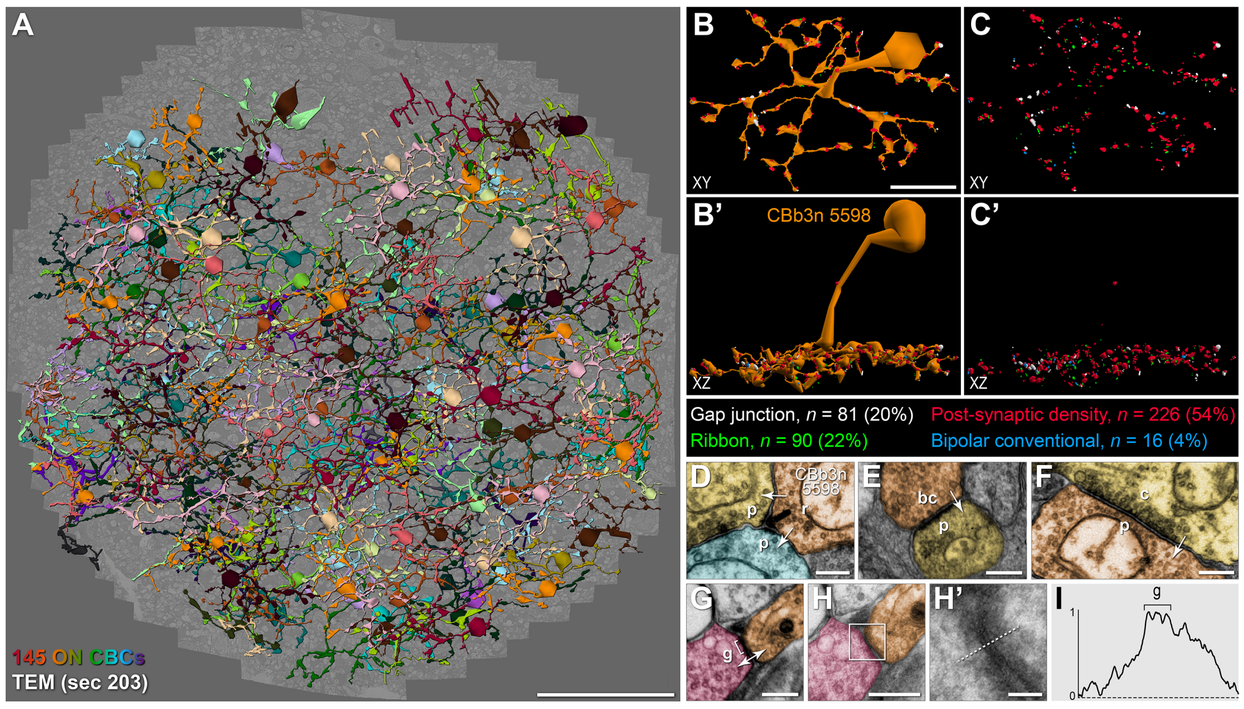

Figure 1. Ultrastructural reconstruction of ON CBCs and their synaptology. RC1 is a 0.25 mm diameter volume of a light-adapted 13-month old female Dutch Belted rabbit retina, built by automated transmission electron microscopy and computational assembly at 2.18 nm/px resolution. ON CBCs and their coupling partners were annotated using the Viking Viewer for Connectomics and their connectivity explored with 3D rendering and network graph visualization leveraging a spatial database and established computational geometry analysis methods. (**A**) 3D computer reconstruction of the 145 ON CBCs contained in RC1 superimposed on a TEM section from RC1. (**B,C**) 3D rendering of CBb3n 5598 and its 413 identified synapses. (**D-G**) Representative examples of synaptic contacts as viewed in the Viking Viewer (native 2.18 nm resolution). (**H-J**) Gap junctions were validated by 0.27 nm resolution recapture with goniometric tilt as necessary. (**I**) Normalized plot of the image density profile taken along dotted line in **H'**. Scale bars: (**A**) 50 µm; (**B**) 10 µm; (**D-H**) 250 nm; (**H'**) 50 nm. Abbreviations: bc, bipolar conventional pre-synapse; c, conventional pre-synapse; g, gap junction; p, post-synaptic density; r, ribbon.

3. *In-class* homocellular coupling produces sheets of coupled cells.

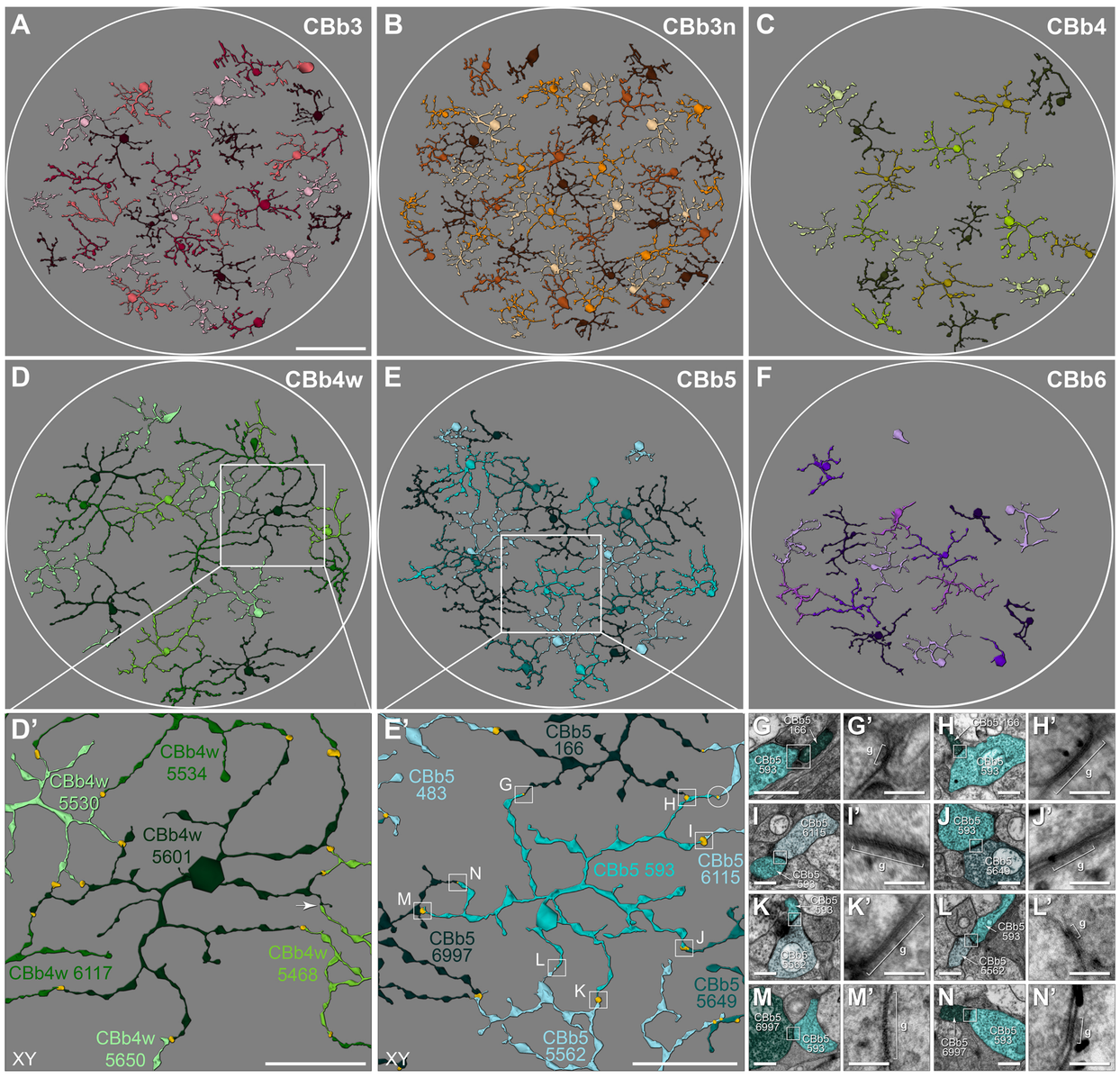

Figure 2. Multipoint coupling within ON CBC classes creates sheets of coupled cells. (**A-F**) 3D computer renderings of the classified ON CBCs in RC1. Axonal arbors within each class jigsaw together to cover the retina optimally, without overlap, a pattern known as *tiling*. In contrast, CBbwf arbors do not tile and exhibit overlap (not shown). Circles approximate RC1 volume boundaries. (**D',E'**) Magnified views of areas in **D,E**. Axonal processes contacting neighbors of the same class terminated in tip-to-tip or tip-to-shaft gap junctions (yellow dots), that mediate *in-class* homocellular coupling. Arrow in **D'** indicates a rare instance of contact without a gap junction. Gap junctions scaled by a factor of 4 (**D'**) or 6 (**E'**) for visibility. (**G-N**) Gap junctions in **E'** confirmed by TEM recapture at 40,000X (0.27 nm/pixel) with goniometric tilt. (**O**) Frequency of *in-class* gap junctions by ON CBC class. Bars depict mean ± SD per cell. Plot includes both confirmed and candidate gap junctions. Gap junctions between processes of the same cell, "self", mediate a type of *in-class* coupling but are not included here. ON CBC classes differed in the frequency of *in-class* coupling instances with neighboring cells. Scale bars: (**A**) 50 µm; (**D',E'**) 20 µm; (**G-N**) 500 nm; (**G'-N'**) 100 nm. Abbreviations: g, gap junction.

4. *Cross-class* homocellular and heterocellular coupling directly or indirectly links specific sheets to differing degrees.

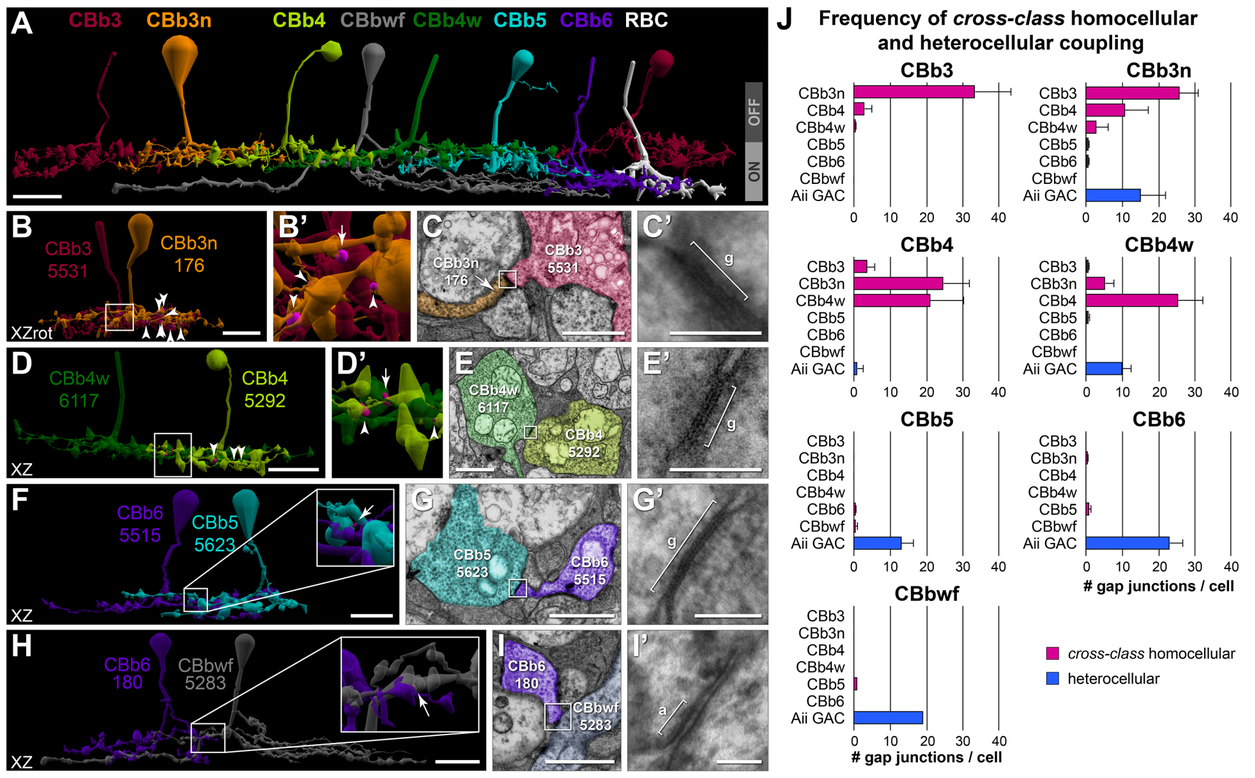

Figure 3. ON CBCs couple with subsets of other ON CBC classes (*cross-class* homocellular) and Aii GACs (heterocellular). (**A**) Extensive co-stratification of ON CBC axonal arborizations. 3D computer renderings of reconstructions of representative members of each ON CBC class from connectome RC1, shown in vertical (YZ) orientation. Cells were chosen based on location to honor relative stratification due to volume curvature and tilt. A rod bipolar cell (RBC) is shown for reference. The CBbwf cell was used to correct for X-axis tilt, while the two CBb3 cells illustrate the Y-axis tilt across the volume. Constructed by overlaying multiple VikingPlot renders, where each rendered all nine cells, but only one cell visible, thereby retaining spatial relationships while removing arbor entwinement for visualization. Cells were translated laterally to further enhance visibility and flipped vertically to achieve the desired ordering. (**B-J**) All classes participate in cross-class coupling, to varying degrees, but not all class pairings couple. (**B,D,F,H**) 3D computer renderings of representative cells illustrating class pairings. Gap junctions mediating *cross-class* coupling (magenta) and adherens junctions (tan) indicated by arrows and arrowheads. Gap junctions scaled by a factor of 4 (**B,D**) for visibility. (**C,E,G,I**) TEM images from the Viking Viewer of gap junctions indicated by arrows in (**B,D,F,H**). (**C',E',G',I'**) Confirmation by TEM recapture at 40,000X (0.27 nm/pixel) with goniometric tilt. (**J**) Frequency of *cross-class* and heterocellular gap junctions by ON CBC class. Bars depict mean ± SD per cell. Plot includes both confirmed and candidate gap junctions. Scale bars: (**A,B,D,F,H**) 10 µm; (**C,E,G,I**) 1 µm; (**C',E',G',I'**) 100 nm. Abbreviations: a, adherens junction; g, gap junction.

5. Specificity exists beyond the contact opportunities afforded by morphology.

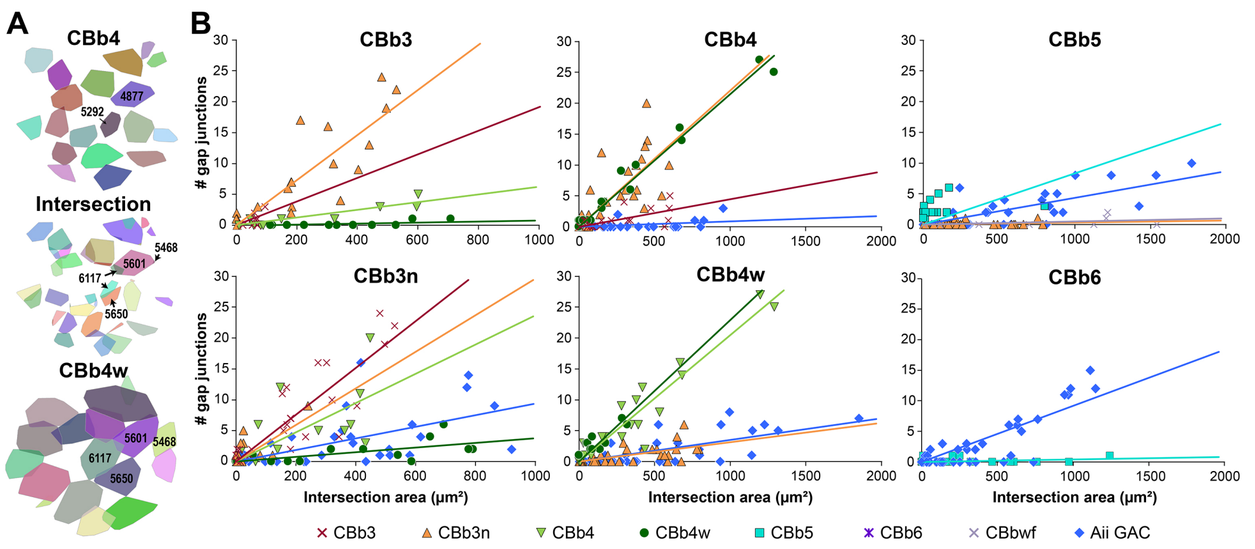

Figure 4. Geometry accounts for the variation in, but not specificity of, ON CBC coupling. (**A**) Spatial results of the SQL query calculating the 2-dimensional (XY) intersection of the convex hulls for each CBb4 cell with that of each member of the CBb4w class. *Top*, Convex hulls of CBb4 cells. *Bottom*, Convex hulls of CBb4w cells. *Middle*, portion of each CBb4 cell's convex hull that intersects in XY with the convex hull of a CBb4w cell. (**B**) Coupling frequency as a function of the degree of axonal field intersection between cell pairings (computed in **A**) for each class. Each point represents a single calculated area of intersection between two cells, regardless of the presence/absence of coupling. Thus, many points have an intersection area > 0, but zero gap junctions. Since each point represents a single cell-cell pairing (ie. CBb4 4877-CBb4w 5601), every cell contributes multiple points due to multiple pairings.

6. Network Summary

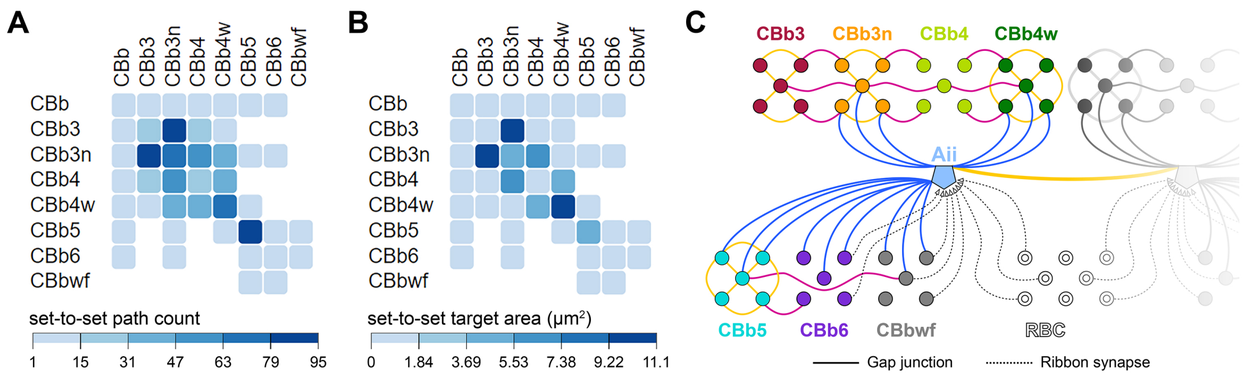

Figure 5. Summary of coupling within and among parallel processing channels of the rabbit retina. (**A**) The connectivity matrix generated by Graffinity summarizing the frequency of single-hop paths between ON CBC classes mediated by gap junctions. Note that the data include all nodes and edges currently annotated in connectome RC1, including incompletely annotated cells and nonvalidated gap junctions. Empty tiles indicate zero identified paths. Each ON CBC class exhibited unique combinations of coupled ON CBC partners. The matrix also highlights the interconnectedness of the highly costratified shallow classes and relative isolation of the deeper classes. (**B**) Connectivity matrix plotted using the cumulative gap junction area to better approximate coupling strength between partner classes. Accounting for the size of gap junctions slightly alters the coupling profiles when compared to frequency alone (**A**). (**C**) *In-* and *cross-class* coupling greatly extends the coupled Aii GAC/ON CBC network. Solid lines show coupling paths (electrical synapses), while dashed arrows show the direction of chemical synapses. Canonical heterocellular coupling (blue) between ON CBCs (circles) and Aii GACs (blue pentagon) is restricted to five of the seven ON CBC classes. *In-class* homocellular coupling (yellow) among neighboring cells of the same class produces sheets of coupled ON CBCs. *Cross-class* homocellular coupling (magenta) connects specific sheets to differing degrees. CBb3 (maroon) and CBb4 (lime) indirectly couple with Aii GACs through direct *cross-class* homocellular coupling (magenta) with CBb3n (orange) and/or CBb4w (green). CBb6 (purple) and CBbwf (gray) uniquely contact Aii GACs with both electrical and chemical (ribbon) synapses, while rod bipolar cells (double circles) connect with chemical synapses only.

7. Conclusions.

Although sparsely distributed, gap junctions formed by ON CBCs are prominent network components, with specificity rivaling that of chemical synapses. These gap junctions not only subserve canonical signal transfer for night vision, but also extensive coupling within and across the parallel processing streams of the retina, producing complex network topologies. Retinal bipolar cells are not spiking neurons but are generally considered electrotonically compact, allowing patches of coupled CBCs to synchronize signals. Thus, coupling likely enhances synchrony to support precise tuning of sustained and transient pathways, or like cone photoreceptors, may mediate signal smoothing, particularly of inhibition, rather than precise timing. Incorporating such coupling topologies into network models is crucial to understanding network function, yet the majority of these gap junctions are inaccessible to light microscopic studies due to their small size.

Support & Disclosures

NIH grants R01 EY028927 and R01 EY015128 (BWJ), R01 EY02576 (REM), T32 EY024234 Vision Training Grant (REM and CLS); P30 EY014800 Vision Core Grant; the Calvin and JeNeal Hatch Presidential Endowed Chair (REM); an unrestricted grant from Research to Prevent Blindness to the Moran Eye Center; and a Research to Prevent Blindness Career Development Award (BWJ). Funding for the JEOL JEM-1400 was generously provided by the late Martha Ann Healy, a friend of the Moran Eye Center.

Research to Prevent Blindness

Robert E. Marc is a principal of Signature Immunologics, Inc., manufacturer of some antibodies used for cell classification in RC1.